Available online at www.sciencedirect.com
SCIENCE DIRECT
ELSEVIER
Polymer 46 (2005) 3372–3384
polymer
www.elsevier.com/locate/polymer

Role of chain entanglements on fiber formation during electrospinning of polymer solutions: good solvent, non-specific polymer–polymer interaction limit

Suresh L. Shenoy[a,*], W. Douglas Bates[a], Harry L. Frisch[b], Gary E. Wnek[a,*,1]

[a]*Chemical and Life Sciences Engineering, Virginia Commonwealth University, 601 West Main Street, P.O. Box 843028, Richmond, VA 23284-3028, USA*
[b]*Department of Chemistry, University at Albany, Albany, NY 12222, USA*

Received 15 December 2004; received in revised form 3 March 2005; accepted 4 March 2005
Available online 25 March 2005

Abstract

Chain entanglements are one of many parameters that can significantly influence fiber formation during polymer electrospinning. While the importance of chain entanglements has been acknowledged, there is no clear understanding of how many entanglements are required to affect/stabilize fiber formation. In this paper, polymer solution rheology arguments have been extrapolated to formulate a semi-empirical analysis to explain the transition from electrospraying to electrospinning in the good solvent, non-specific polymer–polymer interaction limit. Utilizing entanglement and weight average molecular weights (M_e, M_w), the requisite polymer concentration for fiber formation may be determined a priori, eliminating the laborious trial-and-error methodology typically employed to produce electrospun fibers. Incipient, incomplete fiber formation is correctly predicted for a variety of polymer/solvent systems at one entanglement per chain. Complete, stable fiber formation occurs at ≥ 2.5 entanglements per chain.

Keywords: Electrospinning; Chain entanglements; Fiber formation

1. Introduction

Electrostatic spinning (electrospinning) has received a great deal of attention in the literature, especially after Reneker and co-workers [1–3] renewed interest in this phenomenon. Since then, numerous polymers have been electrospun to make fibers [4], and a comprehensive list of these spun fibers has been compiled in a recent review [5]. The ability to make ultrafine electrospun fibers makes it attractive for applications such as wound dressings [6], filtration [7,8], drug delivery [9], protective clothing for the military [10,11] and tissue scaffolds [12–14].

During the electrospinning process, under the application of an electric field a drop of polymer solution is presented at the spinneret tip. As the intensity of the electric field is increased, mutual charge repulsion on the drop surface increases, dramatically altering the droplet shape to form a Taylor cone [15]. Eventually, charge repulsion exceeds surface tension and a jet of solution is ejected from the Taylor cone towards the grounded target substrate. During jet acceleration towards the substrate, substantial solvent evaporation leaves behind polymer fibers in the form of non-woven mats. Frequently, the jet undergoes a whipping process during acceleration, which stretches the fiber and significantly reduces fiber diameter [16,17]. This allows fabrication of nanofibers even though needle diameters may be on the order of 0.5 mm.

Though the electrospinning set-up is fairly straightforward, for widespread commercial viability many important questions need to be resolved including: (a) what parameters control the fabrication of fibers as opposed to beads (as in the case of electrospraying)? (b) can fibers of uniform diameter be consistently obtained? (c) can the process be readily scaled up? (d) what are the mechanical properties of these fibers or fiber mats in comparison to bulk polymer? (e) how does the orientation of the fibers compare to

* Corresponding authors. Tel.: +1 804 440 6714; fax: +1 804 828 3846.
E-mail addresses: sshenoy@vcu.edu (S.L. Shenoy), gew5@case.edu (G.E. Wnek).
[1] Present address: Department of Chemical Engineering, Case Western Reserve University, Cleveland, OH 44106-7217, USA.

0032-3861/$ - see front matter © 2005 Elsevier Ltd. All rights reserved.
doi:10.1016/j.polymer.2005.03.011

conventional fibers? and (f) what parameters influence fiber surface morphology? Based on empirical evidence, the many parameters which affect and/or control the process of electrospinning and subsequent fiber morphology are known to be: (1) solution concentration, (2) polymer molecular weight, (3) solution viscosity, (4) solution conductivity, (5) solution surface tension, (6) applied voltage, (7) distance of source electrode from the target substrate, (8) electric field, (9) solution flow rate, (10) temperature, (11) humidity and (12) solvent volatility (see for example Ref. [18]). However, not all the variables mentioned above are fundamental control parameters nor are they independent of each other. For example, solution viscosity is a function of both concentration and polymer molecular weight (among other factors) [19]. In addition, applied voltage, target distance and electric field are all interrelated, as are target distance and solvent volatility.

Several groups have attempted to model the electrospinning process with varying amounts of success [16,17,20–29]. In these models, the electrospinning process is described as an electrohydrodynamics problem, and attempts are focused on modeling the fiber diameter as a function of the distance from the spinneret tip (or more precisely the tip of the Taylor cone). In general, these studies assume a spinnable fluid and are attempting to predict the jet diameter and bending instability process, which is responsible for generating nanoscale fibers. From a fundamental perspective, electrospun fiber diameters and morphologies are a function of solution properties (polymer concentration and molecular weight) and dynamic parameters (solvent volatility, elongational viscosity, jet velocity and flow rate) [29,30]. Utilizing the dynamic approaches above has resulted in accurate modeling of the jet instability and diameter (in particular, see Refs. [17,26,27]). However, predicting the onset of fiber formation has not been examined to our knowledge. Frequently, the necessary conditions or a 'how-to' recipe for electrospinning a particular system is presented in an empirical fashion. We believe that concepts developed for conventional fiber spinning represent valuable background for a discussion of electrospinning, and briefly turn our attention to conventional spinning.

Among the various fiber spinning processes, electrospinning is comparable to conventional dry spinning since both processes involve polymer solutions and the removal of solvent in a gaseous environment. Arguments can be made for flash spinning to be even more relevant [31,32]; unfortunately, there is insufficient background/theoretical work on this process to make a full comparison at this time. In general, for conventional fiber spinning, 'spinnability' of the polymer solution (or melt) refers to the regime in which continuous uniform filaments are obtained [33]. In particular, instability of the extrudate during traditional fiber spinning arises from two effects: (i) capillary wave breakup (Rayleigh instability) and (ii) breakage of the fiber due to the stresses overcoming some limiting tensile strength (cohesive, brittle fracture). The spinnable regime would then occur when there are sufficient forces holding the jet together to overcome the capillary instability (lower spinnability limit). On the other hand, sufficient relaxation time (or low enough strain rates) is necessary for the material to behave in a viscoelastic manner and avoid fracture (upper spinnability limit). Note that fiber breakage due to fracture is less problematic in solution spinning in comparison to melt spinning. Nevertheless, there is an optimum range of the stabilizing forces, between which the jet is prevented from breaking into droplets (Rayleigh instability) while avoiding fracture. Although electrospinning does differ from dry-spinning in some significant ways (e.g. higher strain rates, 'whipping' draws fibers not tension, ambient temperatures, no die-swell and much thinner fibers), the fundamental instabilities that lead to formation of beaded fibers and/or fiber breakage are the same. From this perspective, electrospinning is a special case of dry spinning.

Assuming the above comparison to be valid, examining the work done on dry spinning models is then a useful exercise. Recently, Gou and McHugh [34,35] performed modeling studies on dry spun cellulose acetate (CA) from acetone. A fundamental assumption for modeling was the presence of an elastically deformable entanglement network above a critical polymer concentration or molecular weight. Their results clearly demonstrated the importance of viscoelasticity for fiber formation. The primary events in the formation of fibers by this process appear to be rapid mass transfer of the solvent and the formation of a 'skin' on the fiber. Although the electrospinning process differs from dry-spinning, these fundamental events, namely a deformable elastic model, rapid mass transfer and skin formation on the fiber surface, are expected to be similar.

Experimental observations in electrospinning confirm that for fiber formation to occur, a minimum polymer concentration is required. Below this critical value, application of voltage results in electrospraying or bead formation primarily due to a Rayleigh instability. At these low concentrations, an insufficiently deformable entangled network of polymer chains exists as discussed for conventional solution spinning above. As the polymer concentration is increased, a mixture of beads and fibers is obtained. Further increase in concentration results in formation of continuous fibers, and although it is not typically reported, at even higher polymer concentrations uniform fibers are no longer produced due to the high solution viscosity. Recently, Gupta et al. [36] and Jun et al. [37] have investigated the effect of molecular weight on continuous fiber formation at a given polymer concentration. Increased chain entanglements and longer relaxation times, a consequence of increased polymer concentration, were thought to be responsible for fiber formation. Previous publications from our laboratory have also stressed the importance of chain entanglements in electrospinning [38]. While the relevance of entanglements is generally accepted,

an analysis of their effect on the resulting morphology has not been reported.

In this regard, the results of Stephens et al. [39] are extremely valuable when discussing the utility of extrapolating solution properties to the onset of fibers. The authors employed real time Raman spectroscopy on an ejected jet to determine the polymer/solvent ratio as a function of distance from the nozzle. They concluded that at approximately 1 cm from the nozzle tip, the polymer/solvent ratio of the ejected jet remains essentially unaltered from the initial ratio in the syringe (note: their system employed tetrahydrofuran, THF, a volatile solvent). Consequently, the polymer concentration that is stabilizing the jet from capillary break-up is not changed much from the solution in the syringe barrel. Presumably, further away from the tip as the solvent evaporates, a considerable increase in polymer concentration, entanglements and elongational viscosity occurs, thereby affecting the viscoelastic properties. These results suggest that solution properties such as polymer concentration and molecular weight significantly affect fiber/bead formation in comparison to other governing parameters (i.e. surface tension and conductivity); however, for modeling the jet and resulting fiber diameter, the other governing parameters have been shown to be significant contributors (for example, see Refs. [20,21,27–29]).

In this paper, a semi-empirical approach is employed to demonstrate that chain entanglements due to increased polymer concentration or polymer molecular weight can play a vital role in fiber formation during electrospinning. Recently, McKee et al. demonstrated the importance of the entanglement concentration on electrospinning process for linear and branched polyesters [40]. Our approach, while similar, allows a priori prediction of fiber/bead formation as a function of concentration and molecular weight for a variety of polymer/solvent systems. In addition, this approach might be applicable to conventional dry spinning process.

2. Background

Our goal is to explore the importance and establish a correlation between chain entanglements and fiber formation in electrospinning from polymer/solvent systems in the good solvent limit. It well known that for a given molecular weight (M), the entanglement density increases with concentration (ϕ_p, volume fraction of polymer) [41]. Alternatively, the same result is achieved at a fixed polymer concentration by increasing M. Both approaches result in a corresponding increase in solution viscosity (η). As a result, identifying η (solution or zero shear viscosity) as the governing parameter in electrospinning is reasonable; however, it is the effect of ϕ_p and M (through chain entanglements) that are the underlying, fundamental variables (in the good solvent, non-specific polymer–polymer interaction limit). For hydrogen-bonded polymers such as polyamides, even in good solvents, the effect of polymer–polymer interactions on solution viscosity may not be neglected. Similarly, as the solvent quality decreases, effects of polymer–polymer interactions on solution viscosity become increasingly important and must be taken into account [41,42].

Before proceeding with the analysis, a comment with regard to viscosity is instructive. The elongational viscosity (not shear viscosity) is most frequently used to describe the rheological properties of the polymer solution/melt as it is more akin to the deformations being applied during fiber spinning. Since electrospinning is analogous to conventional fiber spinning, the use of elongational viscosity is more appropriate than zero shear viscosity, and in fact, has been recently done by Feng [29]. However, both zero shear and elongational viscosities are a function of the number of chain entanglements (among other factors). Thus a semi-empirical analysis to correlate fiber formation in electrospinning with the number of entanglements will provide a starting point for future research. Subsequent sections provide a brief review of the entanglement effect in melts and solutions and then apply these concepts to the electroprocessing of polymer solutions.

2.1. Entanglements in polymer melts and solutions

Chain entanglements in a melt are essentially the physical interlocking of polymer chains, which is a direct consequence of chain overlap. In a polymer melt, chain overlap, and hence the number of entanglements (or alternatively entanglement density), increases with polymer chain length or molecular weight, M. This is reflected by the dependence of zero shear melt viscosity, η_0, on the molecular weight. At low molecular weights, in the absence of chain entanglements, η_0 is directly proportional to M. Above the critical molecular weight, M_c, corresponding to one entanglement per chain, a distinct upturn in the η_0 versus molecular weight plot is observed [19,41]. The molecular weight dependence of η_0 changes from M^1 to $M^{3.4}$. Without going into details, it suffices to reiterate that M_c refers to the molecular weight corresponding to the onset of entanglement behavior in η_0 while M_e, the entanglement molecular weight, corresponds to the average molecular weight between entanglement junctions (or couples). It is worth noting that physical chain entanglements behave in a similar manner as chemical cross-links, although the chains can slide past one another affecting viscoelastic behavior. Typically, entanglement molecular weights are obtained by viscosity, plateau modulus and/or steady state compliance measurements [19,41]. From a theoretical perspective, Bueche concluded that the ratio of M_c/M_e, corresponding to the number of entanglements, n_e, is ~ 2 [43]. In general, for most polymers, experimental observations suggest this ratio, M_c/M_e, is between 1.7 and 3 [41].

In a polymer solution, both concentration or volume

fraction ϕ and molecular weight M affect the number of chain entanglements. In a dilute solution, below the critical value c^*, chain overlapping is absent. As a result, there are no chain entanglements. At $c = c^*$, chain overlap is initiated and the number of chain entanglements is proportional to c. In general, a relationship between the entanglement molecular weight in solution, $(M_e)_{soln}$, and the melt, M_e, can be made by utilizing the polymer volume fraction (ϕ_p) such that $(M_e)_{soln} = M_e/\phi_p$, which has been validated by numerous experimental observations [19,41]. The critical molecular weight corresponding to the zero shear viscosity follows a similar relationship. The primary effect of solvent is one of dilution. Since the solution concentrations are well above the dilute solution regime ($c \gg c^*$), the effect of solvent quality as expressed using the Mark–Houwink parameter has been neglected in this analysis [41]. Finally, analogous to polymer melts, the solution viscosity exhibits a sharp upturn at a critical molecular weight $(M_c)_{soln}$ where $(M_c)_{soln}/(M_e)_{soln} \sim 2$.

The solution entanglement number $(n_e)_{soln}$ is defined as the ratio of the polymer molecular weight to its solution entanglement molecular weight, i.e. $(n_e)_{soln} = M/(M_e)_{soln}$. For polydisperse systems, the weight-average molecular weight, M_w, is typically used as the molecular weight. Note that for systems with large polydispersity values, arguments for employing the third-moment average molecular weight, M_z, have been made [44]. Accordingly for moderately concentrated or concentrated solutions (i.e. $c \sim c^*$ and $c \gg c^*$, respectively), the entanglement number in solution $(n_e)_{soln}$ can be determined from Eq. (1), below.

$$(n_e)_{soln} = \frac{M_w}{(M_e)_{soln}} = \frac{(\phi_p M_w)}{M_e} \quad (1)$$

The arguments dealing with zero shear viscosity and molecular weight dependence are expected to remain the same; therefore, the upturn in η_0 (M_w^1 to $M_w^{3.4}$) occurs for $(n_e)_{soln} \sim 2$. However, the number of entanglements per chain is given by $(n_e)_{soln} - 1$, since an entanglement necessarily involves two chains. Consequently, at $(n_e)_{soln} = 2$, there are two entanglements, but only one entanglement per chain.

2.2. Role of entanglements in electroprocessing of polymer–solvent mixtures

During the electroprocessing of polymer solutions, it has been established that an increase in polymer concentration results in the following progression of observed fiber morphology: (1) beads only, (2) beads with incipient fibers, (3) beaded fibers, (4) fibers only and (5) globular fibers/macrobeads. The formation of chain entanglements has been acknowledged as the primary effect in this progression. Fundamentally, electrostatic spraying and spinning of polymer solutions are identical processes with an obvious difference—electrospraying generates droplets/microbeads whereas electrospinning results in fibers. Why is there such a difference in the resulting polymer morphology? Examining the conditions employed for both processes provides a simple explanation: polymer chain overlap is minimal for electrospraying solutions ($c \ll c^*$). From the perspective of the electrospraying community, limiting chain entanglements will help generate smaller droplets and more uniform microbeads. For example, Festag et al. examined the mechanism of inhibiting drop subdivision for dilute polystyrene (PS) solutions [45,46]. Chain entanglements within the drop eventually limit the subdivision of these drops. The mechanism for this process is straightforward. As the solvent evaporates, two competing effects occur: (i) polymer concentration increases and entanglements commence, which stabilizes the droplet from further subdivision and (ii) surface charge increases, which overcomes the droplet surface tension providing a driving force for droplet subdivision. A third factor not to be overlooked is heat transfer due to the rapid evaporation of solvent. This effect will also tend to limit the droplet size: as the droplet is cooled, solvent evaporation slows, skin formation stabilizes the droplets, and surface charge no longer increases.

As the polymer concentration is increased ($c \sim c^*$), a mixture of fibers and beads are observed. In this regime, insufficient chain entanglements are present to fully stabilize the jet. In theory, at even higher polymer concentrations ($c > c^*$), increased chain entanglements can temporarily serve to stabilize the electrospinning jet by inhibiting jet breakup. For dry spinning it has been suggested that above a critical dope (polymer) concentration, the dynamic 'short range' network in the spinning solution is converted to a more stable elastically deformable 'long range' network as the solvent evaporates [34,35,47]. In other words, 'spinnable' solutions exhibit elastic properties [33]. In electrospinning, the existence of a similar mechanism may be invoked. An additional consequence of solvent evaporation is cooling of the jet, which facilitates skin formation and ultimately fiber stabilization. From a fundamental perspective, it is important to understand and be able to predict both the minimum number of entanglements ('short range' entanglement network) in the spinning solution for both fiber initiation (fibers + beads) and complete fiber formation (only fibers). However, since chain disentanglement in the strong elongational flow field is occurring at the same time, exactly how many entanglements are required (so as to form the 'long range' entanglement network as solvent evaporates) is uncertain and is the subject of this paper.

It is here that our previous discussion on the polymer solution viscoelastic behavior is helpful. To recap, as polymer concentration decreases, $(M_e)_{soln}$ increases due to a dilution effect. The solution entanglement number, $(n_e)_{soln}$, can be readily calculated from Eq. (1). The zero shear viscosity exhibits an upturn (M^1 to $M^{3.4}$) for $(n_e)_{soln} \sim 2$, which implies that at least one entanglement per chain is necessary for the viscosity increase. In many instances, the

actual viscosity upturn is a gradual process and begins at $(n_e)_{soln} \leq 2$ and is not finished until $(n_e)_{soln} > 2$. Still, if the fiber initiation can be correlated with a value of $(n_e)_{soln}$ for a variety of polymer/solvent systems and complete fiber formation is also correlated with $(n_e)_{soln}$, then spinnable solutions may be prepared on the basis of a simple calculation.

In subsequent sections, we have used experimental data to show a correspondence between $(n_e)_{soln}$ and fiber formation. The systems chosen for this study are (a) polystyrene (PS)/THF [48], (b) poly(ethylene oxide) (PEO)/H_2O [22,49], (c) poly(D,L-lactic acid) (PDLA)/dimethylformamide (DMF) [50], poly(L-lactic acid) (PLLA)/dichloromethane (DCM) [37], PLLA/chloroform ($CHCl_3$), PLLA/1,1,2,2-tetrachloroethane ($C_2H_2Cl_4$), and (d) poly(vinyl pyrrolidone) (PVP)/ethanol (EtOH). The broad choice of systems allows us to validate our assertion that fiber formation is controlled by $(n_e)_{soln}$ regardless of polymer polarity (non-polar PS versus polar PEO, PVP or PLLA) and even in the presence of strong polymer–solvent interactions (e.g. PEO/water hydrogen bonding). Table 1 lists the entanglement molecular weights for the relevant polymers.

3. Results

3.1. PS/THF

Polystyrene is an amorphous polymer with a glass transition temperature (T_g) around 100 °C. Megelski et al. obtained PS fibers by electrospinning from a variety of solvents including THF [48]. Here, the portion of their results relevant to this study is used. The weight-average molecular weight of PS was 190k (190×10^3gm/mol). The paper provides detailed optical micrographs of bead/fiber formation at 18, 20, 25, 30 and 35 wt% PS, respectively. At 18 wt%, the resulting electroprocessed mats consists of beads only. At 20 wt% PS, structure consisted predominantly of beads with a few incipient fibers. Higher polymer concentrations (25 and 30 wt%) resulted in larger fiber/bead ratios. And finally, at 35 wt%, only fibers were obtained. Therefore, the transition from electrospraying to electrospinning is initiated between 18–20 wt% and completed by 35 wt%.

Employing Eq. (1), the relationship between the calculated $(n_e)_{soln}$ and the transition from electrospraying to electrospinning is evaluated. The entanglement molecular weight of PS is given in Table 1 and obtained from Fetters et al. [51]. Prior to using the values given by Fetters, a correction ($M_e \times 5/4$) is applied to account for the differences in definition of entanglement spacing (Ferry versus Fetters), as suggested by Larson et al. [30]. Thus, M_e of PS is 16.6k, which is in good agreement with the values reported in the literature [19,41]. Fig. 1 plots the calculated $(n_e)_{soln}$ as a function of PS concentration (converted from ϕ_p to wt%) for different molecular weights (50–300k).

Focusing on the 190k plot, three distinct morphology regimes are indicated in Fig. 1: (i) beads only, (ii) fibers + beads and (iii) fibers only. Below 20 wt%, $(n_e)_{soln} < 2$, only beaded morphology is predicted (and observed). It is important to reiterate that experimental observations exhibit a gradual upturn in the viscosity versus M_w (M^1 to $M^{3.4}$), not an abrupt transition. Accordingly, though the transition in Fig. 1 at $(n_e)_{soln} = 2$ is shown as a dotted line, the actual change in morphology from beads to fibers + beads is not as sharp as indicated. In fact, one observes a gradual transformation from beads to elongated beads to a mixture of fibers + beads. Likewise, the transition from fibers + beads to fibers only is a gradual process as less and less beads are observed. At 20 wt% PS, the calculated $(n_e)_{soln}$ is two, which corresponds to an upturn in zero shear viscosity (onset of entanglements). This correlates with the experimental observation of fiber initiation. Even though fiber formation is initiated around 20 wt% PS (corresponding to one entanglement/chain), this is not enough for complete jet stabilization, especially under the influence of the strong elongational flow field. In fact, the observation of fibers and beads for concentrations up to 30 wt% PS supports the

Table 1
Entanglement molecular weights of the polymers considered in this study

Polymer	Entanglement molecular weight ($M_e \times 10^3$ g/mol)
Polystyrene (PS)	16.6
Poly(ethylene oxide) (PEO)	2.1
Poly(L-lactic acid) (PLLA)	8.0
Poly(vinylpyrrolidone) (PVP)	16.8 (estimated)

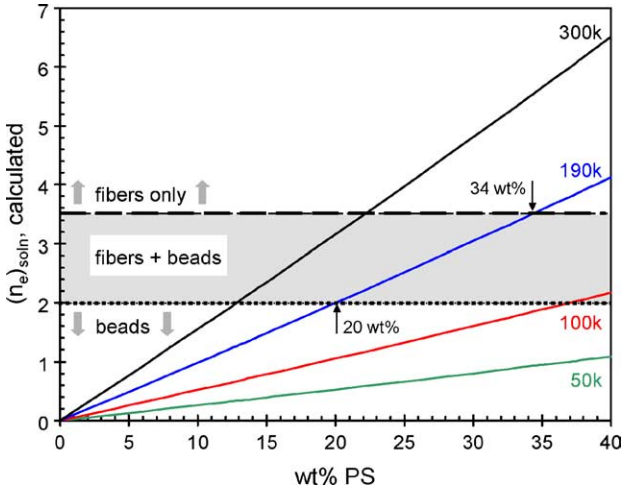

Fig. 1. Plot of the calculated entanglement number $(n_e)_{soln}$ (Eq. (1)) as a function of concentration for PS/THF system. The dashed line indicates the transition for complete fiber formation, i.e. $(n_e)_{soln} = 3.5$, while the dotted line indicates the boundary between beads and a mixture of fibers and beads (shown in fill). Each line represents a different weight-average molecular weight (M_w): 50, 100, 190 and 300k. Arrows indicate the onset of fiber formation (20 wt%) and complete fiber formation (34 wt%) for 190k sample, in agreement with observations (Table 2).

hypothesis of insufficient entanglements for jet stabilization. Continuing further, when the PS concentration is increased to 35 wt%, only fibers are obtained, which corresponds to $(n_e)_{soln}=3.5$ or 2.5 entanglements/chain. The arrow at 34 wt% in Fig. 1, indicates this last transition.

The effect of molecular weight on calculated fiber onset and fiber only transitions is clearly indicated by comparing the 50, 100, 190 and 300k calculations, which show much lower concentration thresholds as the M_w is increased. Moreover, by simply using the entanglement molecular weight (M_e) of the undiluted PS, the electrospinning concentration regime of a known molecular weight PS sample may be predicted and correlated with the onset of entanglements. The more significant question is whether this analysis (based exclusively on chain entanglements) can be applied to other polymer solutions. Moreover, since PS is a non-polar polymer, will this analysis be applicable to polar polymers as well? In an attempt to answer these questions, the semi-empirical entanglement analysis was applied to other systems. The results of the analyses including that of PS/THF are tabulated in Table 2. Also provided in Table 2 are the experimental data for fiber initiation and complete fiber formation obtained from the literature for these systems.

3.2. PLA/DMF or PLA/DCM

Poly(lactic acid), PLA, is a biocompatible/biodegradable linear aliphatic polyester. PLA can be completely amorphous as in the case of poly(D,L-lactide) (PDLA) or semi-crystalline in the case of poly(L-lactide) (PLLA). Zong et al. [50] investigated the effect of processing parameters to make electrospun, bioabsorbable non-woven PDLA membranes for biomedical applications. The weight-average molecular weight of PDLA was 109k and DMF was employed as the solvent. The authors observed that at concentrations <20 wt%, a mixture of large beads and fibers was generated, whereas only fibers were generated on electrospinning solutions between 30 and 35 wt%. Recently, Jun et al. have explored the various parameters important for electrospinning of semi-crystalline PLLA fibers [37]. Dichloromethane (DCM) was the solvent and the polymer molecular weight was 670k (M_w). In contrast to the results of Zong, a mixture of fibers and beads were obtained at concentrations ≤ 1 wt%, and for concentrations ≥ 3 wt%, only fibers were observed. The authors speculated that the large difference in the polymer concentrations required for fiber initiation and complete fiber formation was probably a consequence of the different solvents employed (and by inference, related to solvent volatility effects, $(T_{BP})_{DMF}=153$ °C versus $(T_{BP})_{DCM}=40$ °C).

While the M_e of PLLA is readily available in the literature, no reports on $(M_e)_{PDLA}$ could be found. As a first approximation, the entanglement molecular weights were assumed to be equivalent, $(M_e)_{PDLA}=(M_e)_{PLLA}=8.0$k [52]. Note, by definition, M_e (average molecular weight between entanglements) is primarily a function of chain geometry (architecture) [19,41]. Consequently, despite the large difference in M_w between PDLA and PLLA (109 versus 670k), our assumption that $(M_e)_{PDLA}\sim(M_e)_{PLLA}$ is reasonable; however, the number of entanglements per chain (or solution entanglement number as defined by Eq. (1)) for PLLA will be significantly higher [53,54]. Using the reported value, the polymer concentrations corresponding to fiber initiation, $(n_e)_{soln}=2$, and complete fiber formation, $(n_e)_{soln}=3.5$, were determined for both PDLA/DMF and PLLA/DCM. As shown in Fig. 2 (tabulated in Table 2), our calculations show that for fiber initiation should occur at $\sim$20 wt% for PDLA (109k) and 2.3 wt% for PLLA (670k) while complete fiber formation is expected at 32 wt% for PDLA and 4 wt% for PLLA. The calculated results are in excellent agreement with the experimentally observed values for both PDLA and PLLA. To ascertain whether the large difference in PLLA and PDLA concentrations is truly a molecular weight phenomenon or a solvent effect as suggested by the authors [37], attempts were made to electrospin high molecular weight PLLA ($M_w=670$k) from DMF. The original intent was to validate the entanglement analysis by electrospinning PLLA/DMF solutions; however, PLLA is insoluble in DMF even at elevated temperatures.

Table 2
Summary of results for various polymer/solvent systems

System polymer/solvent	M_w ($\times 10^3$) g/mol	Polymer concentration (wt%) estimated by entanglement analysis		Polymer concentration (wt%) observed experimentally	
		Fiber initiation (fibers + beads) $(n_e)_{soln}\sim 2$	Fibers only $(n_e)_{soln}\sim 3.5$	Fiber initiation (fibers + beads)	Fibers only
PS/THF [48]	190	20	34	18	30–35
PDLA/DMF [50]	109	18.5	32	<20	30–35
PLLA/DCM [37]	670	2.3	4	<1	3
PLLA/$CHCl_3$	670	2.0	3.5	–	<4.1
PLLA/$C_2H_2Cl_4$	670	1.9	3.4	<3	>4
PEO/H_2O [56]	400	1.5	2.5	NR	4
PEO/H_2O [20]	2000	0.3	0.8	NR	<2
PVP/EtOH	1300	4	7.5	3	7–9

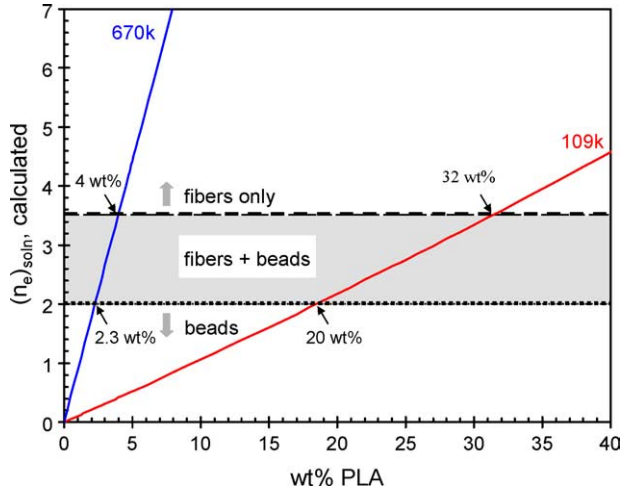

Fig. 2. Plot of the calculated entanglement number $(n_e)_{soln}$ (Eq. (1)) as a function of concentration for PLA/(DMF/DCM) systems. The dashed line indicates the transition for complete fiber formation, i.e. $(n_e)_{soln}=3.5$, while the dotted line indicates the boundary between beads and a mixture of fibers and beads (shown in fill). The lines represent the samples with $M_w=670$ and 109k, and arrows indicate the onset of fiber formation (2.3 and 18.5 wt%) and complete fiber formation (4 and 31 wt%) for the 670 and 190k samples, respectively.

Nevertheless, based on preliminary electrospinning experiments performed in other chlorinated solvents of differing volatility [55], it appears that the variation in the critical concentration between the studies of Jun and Zong may be attributed to the large M_w differences (670 versus 109k) of the samples more than differences in solvent volatility. Still, the extreme volatility of DCM may make a minor contribution to the observation of fiber onset at lower concentrations.

3.3. PEO/H_2O

Polyethylene oxide is a semi-crystalline linear aliphatic polyether with a low T_m (65 °C). Dietzel et al. [56] have examined the effect of processing variables including concentration on electrospinning of PEO in H_2O. The authors observed that for 4–10 wt% PEO ($M_w=400$k) only fibers were produced. Below this critical concentration (4 wt%), a mixture of fibers and beads were obtained. In another study by Shin et al. [22], 2 wt% PEO ($M_w=2000$k) was deliberately chosen to ensure that only fibers were produced, which implies the critical concentration corresponding to complete fiber formation is <2 wt%. The PEO/H_2O system gives us an opportunity to apply the entanglement analysis, where strong polymer/solvent interactions (hydrogen bonding between PEO ether groups and hydroxyl groups in H_2O) are known to exist.

Table 1 gives $(M_e)_{PEO}$ obtained from literature [51] by applying the proper correction ($M_e\times5/4$). The comparison between experimental data and predicted values are given in Table 2. Entanglement analysis predicts that for $M_w=400$k, and concentrations >2.5 wt% only fibers should be obtained, while for a 2000k sample the corresponding concentration is 0.8 wt%. Experimentally, Deitzel et al. observed a critical concentration of 4 wt%—whether the presence of strong specific interactions between PEO and H_2O is the cause of this discrepancy between calculated and observed fibers is unclear at this time. In addition, fiber initiation is expected to be at ~1.5 wt%, which cannot be confirmed since the authors did not report the PEO wt% for fiber initiation. For the 2000k sample, at 2 wt%, the concentration employed by Shin, one is well above minimum concentration for complete fiber formation. The concentration for fiber initiation is predicted to be ~0.3 wt%. Hence, a mixture of fibers and beads should be obtained for concentrations between 0.3 and 0.8 wt% PEO. Lacking experimental data to confirm this prediction, validation of predicted fiber onset was attempted by electrospinning a 0.4 wt% PEO solution ($M_w=2000$k) in H_2O [57]. Electrospinning predominantly resulted in bead formation; however, close inspection of the glass slide showed some incipient fibers, which consisted of beads attached to one another (Fig. 3). At this low concentration, PEO beads cover most of the slide. Evidently, 0.4 wt% PEO/H_2O solutions are near the threshold for fiber onset in agreement with the entanglement analysis.

The simple entanglement analysis clearly demonstrates that the viscosity transition, i.e. $(n_e)_{soln}\sim2$, corresponds to fiber initiation while $(n_e)_{soln}\sim3.5$ corresponds to complete fiber formation. In addition, this analysis is valid not just for non-polar polymer/solvent systems but also where polymer–solvent hydrogen bonds are involved. The good agreement between the experimental observations and the predictions clearly illustrate the role played by entanglements in the electrospinning process for the good solvent case. So far, this approach has been validated using experimental observations published in the literature on polymers with reported M_e values. In the next section (and as a further test of this approach), a system for which no prior detailed experimental data are available is examined (including no reported M_e values).

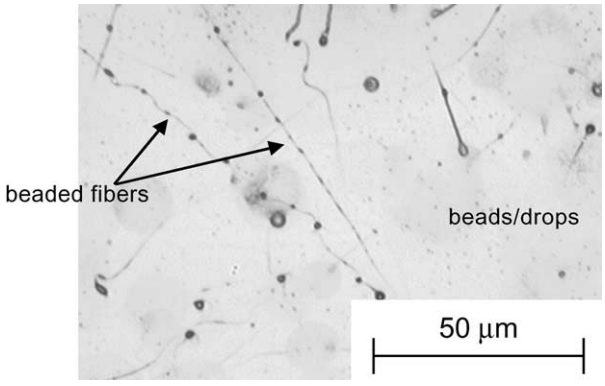

Fig. 3. Optical micrograph of the structures obtained by electrospinning 0.4 wt% PEO ($M_w=2000$k) in deionized H_2O. Note the presence of beads and beaded fiber morphology.

3.4. PVP/EtOH

Poly(vinyl pyrrolidone) is an amorphous polymer that may form hydrogen bonds to protic solvents such as alcohols. Recently, Yang et al. [58] and Li et al. [59] obtained fibers by electrospinning PVP in EtOH, DMF and an EtOH/DMF mixture. However, in both instances, no information on the concentration dependence of fiber initiation and/or fiber formation was presented. Consequently, the PVP/EtOH system was chosen to provide further substantiation of the entanglement analysis. In the absence of any report on the entanglement molecular weight for PVP, $(M_e)_{PVP}$, an estimated value of $(M_e)_{PVP}$ was determined using the entanglement constraint model [51]. According to Fetters, the M_e of a polymers is a function of the characteristic ratio (C_∞), the average molecular weight per backbone bond (m_o), bond length (l_o) and density (ρ). The precise dependence is given in Eq. (2), below:

$$M_e \propto C_\infty^{-3} m_o^3 l_o^{-6} \rho^{-2} \quad (2)$$

Using the above relationship, the value of the $(M_e)_{PVP}$ can be estimated by comparing to a reference polymer possessing similar topological structure. In this case, PS is chosen as the reference thereby eliminating l_o as a variable (since $(l_o)_{PS} \sim (l_o)_{PVP}$). The characteristic ratios of PVP reported in the literature have generally been obtained in solution and vary significantly [60,61]. For example, $C_{\infty(PVP/H2O)} = 14$ while $C_{\infty(PVP/EtOH–H2O)} = 12.3$; in this case, the calculated value of $C_{\infty(PVP)} \sim 11$ is selected [61]. Other parameters employed for the calculation (Eq. (2)) include $C_{\infty(PS)} = 10.8$; $\rho_{PS} = 1.06$ g/cm^3; $\rho_{PVP} = 1.13$ g/cm^3 [62]. Employing $(M_e)_{PS} = 16.6$k as given in Table 1, $(M_e)_{PVP}$ was estimated using Eq. (2) to be 16.8k. The similarity of the M_e values for PS and PVP is not surprising since chain entanglements are predominantly a function of topology. Using $M_w = 1300$k, Eq. (1) is employed to calculate the polymer concentration required for fiber initiation and complete fiber formation and is reported in Table 2. Accordingly, fiber initiation is predicted to commence at 4 wt% while only fibers should be obtained for PVP concentrations ≥ 7.5 wt%. Between these two concentration limits, a mixture of fibers and beads is predicted.

Based on these calculations, PVP/EtOH solutions with 1, 3, 7 and 9 wt% polymer, respectively, were prepared and electrospun while keeping the other control parameters such as applied voltage, flow-rate and source-to-target distance constant [57]. Optical micrographs in Fig. 4 clearly show at 1 wt% polymer (Fig. 4(A)), the structure is predominantly one of elongated beads. As PVP concentration is increased to 3 wt% (Fig. 4(B)), the presence of a few electrospun fibers becomes apparent though the dominant morphology is beads. Thus fiber initiation occurs around 3 wt% that is in reasonable agreement with the predicted value (4 wt%). At 7 wt% (Fig. 4(C)), the morphology is essentially fibers, with some fibers having a beaded morphology. The critical concentration for complete fiber formation is slightly higher than 7 wt%, which does not corroborate the results of Yang wherein smooth nanofibers of PVP in EtOH were obtained at 4 wt% [58]. To eliminate electric field as a possible reason for this discrepancy, the effect of electric field on fiber morphology for a concentration of 7 wt% was examined (not shown in figure). Beaded fiber morphology was obtained for voltages from 12 to 20 kV keeping the source-to-target distance constant at 12 cm. A probable cause for the disagreement could be the mode of collection of the fibers/beads [63]. An alternative explanation might be the presence of titanium tetraisopropoxide in the solutions used by Yang, which could alter the critical concentration for complete fiber formation. However, at the present time, this is purely speculative and the precise reason(s) for the discrepancy is still not fully resolved. In our case, as the PVP concentration is increased to 9 wt%, a completely fibrous network is obtained as shown in Fig. 4(D). This is in excellent agreement with calculations. Summarizing, fiber initiation occurs around 3 wt%, from 3 to 7 wt% a mixture of fibers + beads are observed, and at 9 wt%, only fibers are obtained. This example clearly illustrates the importance of the entanglement analysis even in the absence of reliable M_e values.

4. Discussion

4.1. Universality of the model

By predicting fiber/bead formation for various systems, the validity of an entanglement analysis is clearly demonstrated. The present analysis requires calculation of $(n_e)_{soln}$, which varies with the molecular weight, M_w. Alternatively, one can employ the Simha–Frisch parameter $= c[\eta]$ (also referred to as the Berry number) to describe the degree of chain overlap in a solution [64]. Recently, Koski et al. [65] employed this type of analysis to predict complete fiber formation. The approach that we have outlined, valid for the good solvent case in the absence of strong interactions permits the prediction of bead/fiber formation apriori without the necessity of any experiments. Furthermore, the dependence of viscosity (chain entanglements in this case) on $c[\eta]$ is believed to be a result of the equivalent sphere hydrodynamics; consequently, it is valid for low polymer concentrations. At higher concentrations, a fundamentally different type of intermolecular interaction dependent on $(\phi_p M_w)$ rather than $c[\eta]$, is more relevant [41]. In electrospinning, the required polymer concentrations are generally in the semi-dilute ($c \gg c^*$) regime; hence the product, $\phi_p M_w$, is more appropriate in this instance. Fig. 5 shows a plot of this type for the PEO/H_2O system. Based on the previously discussed value of $(n_e)_{soln} \sim 2$, the graph predicts that a mixture of fibers + beads is obtained as long as $\phi_p M_w \geq 4.2$k. On the other hand, for $\phi_p M_w \geq 7.4$k, the

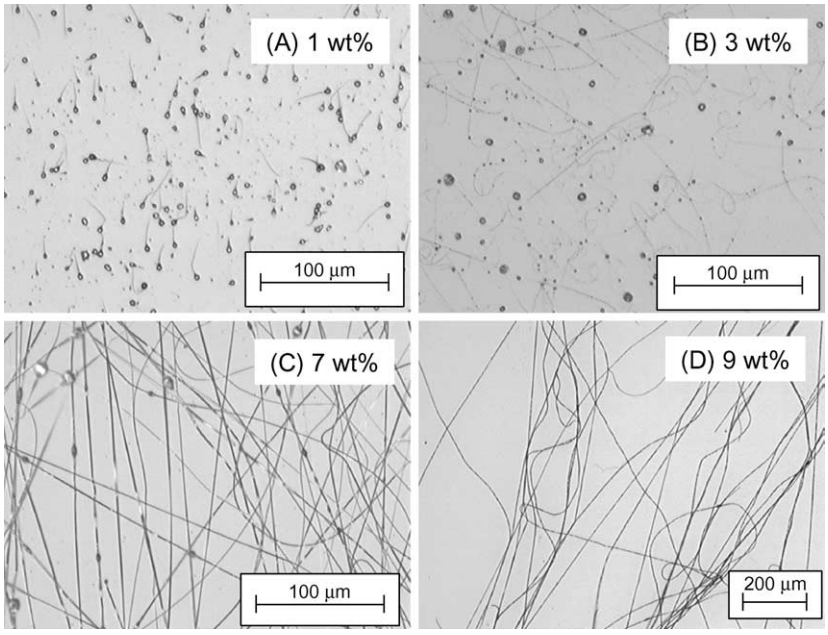

Fig. 4. Optical microscopy of structures obtained by electrospinning PVP/EtOH solutions at different concentrations of PVP (M_w = 1300k). (A) 1 wt%, elongated beads; (B) 3 wt%, incipient fiber formation; (C) 7 wt%, beaded fibers and fibers; and (D) 9 wt%, fibers only.

graph predicts only fibers should be obtained, which is confirmed by experiment. Therefore for PEO/H_2O electrospinning, the value of $\phi_p M_w$ (7.4k) at which the electrospraying to electrospinning transition occurs implies that the critical PEO concentrations can be prepared with just the knowledge of the weight-average molecular weight of PEO. These critical $\phi_p M_w$ values are valid for PEO only (since the slope of the line in Fig. 5 is $1/M_e$), but similar plots can be developed for other polymers.

One way to standardize the above treatment for other polymers may be by using the definition of $(n_e)_{soln}$. For initiation of fibers, i.e. $(n_e)_{soln} = 2$, and $\phi_p M_w = 2M_e$. On the other hand, for complete fiber formation, $(n_e)_{soln} \geq 3.5$, or $\phi_p M_w \geq 3.5\ M_e$. Thus with the knowledge of the entanglement molecular weight (M_e) and the weight-average molecular weight (M_w) for a given polymer, one may predict a priori the polymer concentrations (ϕ_p) required to move through the electrospraying/electrospinning transition.

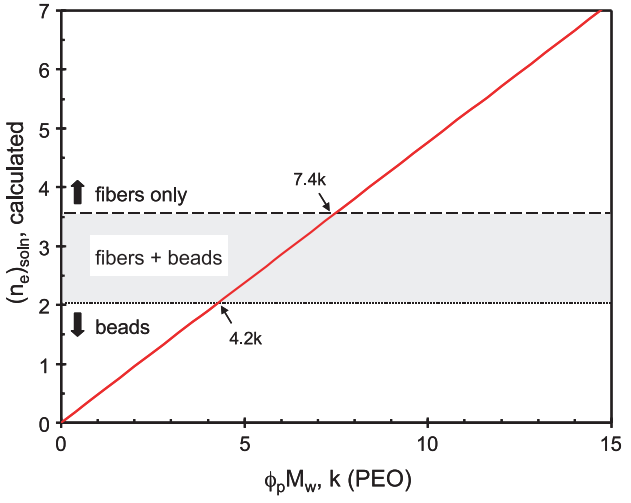

Fig. 5. Calculated $(n_e)_{soln}$ for PEO/H_2O as a function of $(\phi_p M_w)$. The slope of the plot is $1/M_e$, and the arrows indicate fiber onset and fiber only morphologies at $\phi_p M_w = 4.2$ and 7.4k, respectively.

4.2. Comments on relationship between $(n_e)_{soln}$ and fiber/bead formation

From a fundamental perspective, as discussed previously in this paper, the volume fraction ϕ_p or molecular weight M_w at which fiber initiation occurs corresponds to the sharp upturn (M_w^1 to $M_w^{3.4}$) in the $\eta - M_w$ plot, i.e. $(n_e)_{soln} \sim 2$ (number of entanglements/chain = 1). Experimental evidence demonstrates that increasing ϕ_p or M_w results in a mixture of fibers and beads. Eventually above a certain critical ϕ_p or M_w value, only fibers are obtained. Our analysis based on experimental data suggests that the $(n_e)_{soln}$ value corresponding to this transition is ~ 3.5, which is equivalent to about 2.5 entanglements/chain. Interestingly, in early work, Schreiber et al. [66] and Hayahara et al. [67] suggested that in polymer melts or concentrated solutions, there exists a critical M_w or ϕ_p, above which an elastically deformable entanglement network is obtained. For concentrated acrylonitrile–methyl acrylate copolymer solutions, it was concluded that the minimum number of entanglements required to form this elastic network is ~ 3 [67], which corresponds to $(n_e)_{soln} \sim 4$. In the electrospinning process, our analysis suggests that chain entanglements appear to stabilize the ejected liquid jet long enough for solvent

evaporation to occur and form an elastically deformable 'long range' network, which ultimately yield fibers. Note that it is well known that for a much more extensive elastic network $(n_e)_{soln} \geq 6$–8, the steady state compliance, J_e^0, becomes independent of M_w [19,41]. Summarizing, in good solvents, fiber initiation corresponds to the onset of entanglements whereas there is a direct correlation between complete fiber formation and the onset of a deformable elastic network due to chain entanglements.

In principle, this could imply the existence of a critical M_w below which fiber formation in good solvents may not be possible by electrospinning despite the presence of three of more entanglements per chain. For example, one can envision low molecular weight polymer solutions with $(n_e)_{soln} \sim 4$ at high polymer ϕ_p, where establishing a deformable elastic network may be difficult due to lower relaxation or disentanglement time (τ_D). It is well known that a long chain (higher M_w) needs more time to disentangle than a shorter chain (low M_w). According to the reptation model, $\tau_D \sim M_w^{3.4}$. This can result in significant entanglement loss for low molecular weight polymers in fast flowing systems or under elongational flow such as occurring in electrospinning [68–70]. A critical parameter, which affects the disentanglement of chains, is the applied strain rate ($\dot{\varepsilon}$). The presence of the physical junctions per se does not ensure formation of a mechanical or elastic network due to chain disentanglement. Only under the influence of a shear stress or elongational flow, as is the case for electrospinning, does there exist a critical strain rate (greater than the disentanglement or reptation time), above which the entanglements or physical junctions act as mechanical effective junctions on short time scales ($> \tau_D$) [71]. An appropriate parameter to include these effects (τ_D, $\dot{\varepsilon}$) is the Deborah number (De) as done by Feng [29]. Finally another factor to consider is the extensibility of the chain between the entanglement junctions [72]. For an equal number of entanglements/chain (e.g. three or more for fiber formation in electrospinning), the extensibility would be lower as M_w decreases, which together with a faster disentanglement time would result in significantly reduced elastic forces. In this situation, beads or beaded fibers may be obtained. Work is currently underway in our laboratory to test this hypothesis.

4.3. Fiber formation: effect of other factors

The entanglement analysis clearly shows that in good solvents chain entanglements can act as a stabilizing influence on the ejected jet promoting fiber formation. However, there are other factors that can influence the fiber formation. Among them, the applied voltage and surface tension are two very important parameters, which affect both the Taylor cone and fiber/bead formation. As a starting point, a dimensionless electrospinning number $Vq/\gamma R^2$, defined as the ratio of the electrical energy (Vq) to the surface free energy (γR^2), is introduced. This ratio was specifically chosen since the electrical energy is the driving force for ejection of the jet from the Taylor cone while the surface free energy is the force opposing the jet ejection. Note that $Vq/\gamma R^2$ is quite similar to the electric Bond number [73,74]. Thus, during the electrospinning process, a jet of liquid is ejected from the Taylor cone if $Vq/\gamma R^2 > 1$, i.e. as the electrical energy (Vq) overcomes the surface free energy (γR^2). In addition to the critical voltage needed for the ejection of liquid from the Taylor cone, it is well known that as the voltage (and hence Vq) is increased, the morphology changes from beads to beaded fibers to only fibers. However, further voltage increase can affect cone stability, which can result in the formation of defective (beaded) fibers [56]. An alternate way to obtain fibers is to lower surface tension (and hence γR^2) by adding a surfactant [75]. Thus, qualitatively, the dimensionless number $Vq/\gamma R^2$ may be used to explain the morphologies obtained by electrostatic processing. However, one needs to be extremely careful in using the electrospinning number since $Vq/\gamma R^2$ may be a function of other parameters such as chain entanglements, solvent volatility, flow rate, humidity, and temperature. An in-depth dimensional analysis is being performed to obtain the precise relationships of the various parameters to the electrospinning number and will be the subject of a future paper. Here we simply present some conceptual arguments on the usefulness of the electrospinning number and importance of other factors for determining fiber formation.

4.3.1. Solution conductivity

Jun et al. have shown that increasing solution conductivity by addition of a salt can significantly aid fiber formation [37]. As discussed earlier, a mixture of fibers and beads was obtained by electrospinning a 2 wt% PLLA ($M_w = 670$k) solution from DCM. However, addition of a salt, such as pyridinium formate (PF), enables fiber formation at lower concentrations. For example, by addition of 0.8 wt% PF (with respect to DCM) to a 2 wt% polymer solution, only fibers were obtained. From the entanglement analysis perspective, at 2 wt%, $(n_e)_{soln} < 2$ and hence we expect only beads. While addition of the salt should not change the entanglement number, it has a positive effect on the electrospinning number. Specifically, the electrical energy (Vq) increases. On the other hand, the change in surface free energy (γR^2) due to change in surface tension is not expected to be significant [37]. Thus fiber formation is promoted at lower concentrations, the stabilizing factor being the increased electrical energy [20,21] and not chain entanglements.

One can also disrupt fiber formation by lowering the electrical energy as done by Fong et al. for PEO/water [76]. The authors investigated the effect of neutralizing ions generated by a corona discharge on the morphology of the PEO fibers. In the absence of the discharge, only fibers were obtained. However in the presence of the discharge, beaded fibers were formed. The amount of beads was proportional

to the corona discharge voltage. In this case as the authors suggest the electrical forces (and hence the electrospinning number $Vq/\gamma R^2$) stabilizing the ejected jet is reduced by the neutralizing ions thereby destabilizing the jet. Note that in both the cases discussed above, though the number of entanglements is unchanged, the electrospinning number is altered due to changes in the electrical energy term.

4.3.2. Solvent quality

While the examples considered in this paper clearly show that chain entanglements are important, it should be reiterated that this is valid for good solvents under normal operating conditions. As mentioned earlier, it was assumed that polymer–polymer interactions are not significant enough to affect solution viscosity. Consequently, solvent quality is not an issue and electrospinning PLLA or PDLA from DMF or DCM does not alter model predictions or experimental observations. However, it has been shown that addition of another solvent can dramatically alter the concentration needed for fiber formation. For example, work in our laboratory by Bates et al. suggests that addition of acetone to a PVDF solution ($M_w = 180$k) in DMF significantly lowers the critical concentration necessary for fiber formation [77]. In this case, acetone is a marginal solvent for PVDF as indicated by the polymer–solvent interaction parameters ($\chi_{PVDF/acetone} = 0$–0.1 versus $\chi_{PVDF/DMF} = -0.4$) [78]. In fact, in pure acetone, fibers can be obtained at concentrations as low as 7.5 wt%. Employing our analysis, a concentration of 30 wt% PVDF is calculated to obtain electrospun fibers (for 180k PVDF in DMF—a good solvent). The issue of solvent quality can be quite complex and is outside the scope of this work. However, here we lay the groundwork for future experiments by summarizing our ideas using the example of a polymer/solvent system previously reported by our laboratory.

Kenawy et al. [38] obtained fibers by electrospinning ethylene vinyl alcohol copolymers containing 56–71 wt% vinyl alcohol in rubbing alcohol (*v*/*v*, 70/30 2-propanol/water). Since the copolymer is partially crystalline, application of heat (80 °C) was a prerequisite to completely dissolve the copolymer and obtain a homogenous solution. After cooling to room temperature, electrospinning results in EVOH fibers. The EVOH/rubbing alcohol solution phase behavior is quite complex since it has been clearly demonstrated that both solid/liquid (crystallization) and liquid/liquid phase separation (upper critical solution temperature, UCST) occurs in this system, albeit quite slowly [79]. In fact, the polymer eventually precipitates if left for any prolonged period at room temperature suggesting complete phase separation. Thus the presence of micro- and/or nanoscopic crystallite junctions or 'embryonic nucleation sites', together with the proximity of the UCST, may in fact promote the electrospinning process and subsequent fiber formation. We have preliminary evidence to suggest that a similar process may occur in the case of PVDF in acetone (except for the absence of UCST) and will report on this work in a forthcoming contribution [80].

Another factor that can promote fiber formation is the enhancement of polymer–polymer interactions due to presence of inter-chain hydrogen bonding [81,82]. This is clearly demonstrated by the fiber formation of low molecular weight Nylons ($M_w < 25$k) at low concentrations (2.5 wt%) in contrast to polymers where no hydrogen bonding is present [81].

4.3.3. Fiber diameter

Another area of interest is the prediction of fiber diameter and more importantly the dependence of this diameter on the concentration/molecular weight space. For a given molecular weight, it is well known that fiber diameter increases with polymer concentration. Similar results are observed for fixed concentrations with increasing molecular weights. From our perspective, we are interested in the ability to a priori predict the concentration/molecular weight space for the spinning of nanometer size fibers as opposed to micron size fibers. Using the entanglement analysis we can now formulate a qualitative picture. For lower molecular weight polymers, to satisfy the entanglement consideration [entanglement number $= (n_e)_{soln} = 3.5$] in order to obtain only fibers, a higher polymer chain concentration per unit volume would be required which leads to lower extensibility. On the other hand, for high molecular weight polymers, due to the length of each chain, a lower chain concentration per unit volume would be needed to satisfy the entanglement consideration. The lower number of chains per unit volume should directly translate to lower fiber diameters due to large chain extensibility. This argument is currently under investigation and results will be reported in the near future. This is conceptually in agreement with the suggestion by McKee et al. [40] who demonstrated that the fiber diameter could be universally scaled with the normalized concentration (to the entanglement concentration) to the 2.6 power.

5. Conclusions

In the present paper, we believe that we have demonstrated the importance of entanglements for fiber formation in polymer/good solvent systems. In addition, we have proposed a straightforward methodology to apriori predict fiber formation in good solvents. The only required parameter is the entanglement molecular weight of the undiluted polymer (M_e). In general, M_e is readily available for a large number of polymers ($\sim$70 or more). Alternatively, in the absence of experimental values, M_e can also be theoretically estimated (as we have done for PVP) by employing the entanglement constraint model. Then, based on the structure requirements (fibers/beads/mixture), our predictions facilitate the proper choice of polymer concentration/molecular weight space.

Acknowledgements

The authors would like to thank Prof John Rabolt and Dr Joseph Dietzel of the University of Delaware for providing information on the absence of solvent evaporation close to the needle. Additionally, the authors would like to thank Prof Gareth H. McKinley for discussions on entanglements and elongational viscosity. We also thank B.I. (Boehringer Ingelheim) Chemicals for donating samples of poly(L-lactide acid) (M_w = 670k). The authors would also like to thank DARPA (Bio-Optic Synthetic Systems Program) and the NASA Office of Space Sciences for generous support.

References

[1] Doshi J, Reneker DH. J Electrostat 1995;35:151–60.
[2] Srinivasan G, Reneker DH. Polym Int 1995;36:195–201.
[3] Reneker DH, Chun I. Nanotechnology 1996;7:216–23.
[4] Frenot A, Chronakis IS. Curr Opin Colloid Interface Sci 2003;8: 64–75.
[5] Huang ZM, Zhang YZ, Kotaki M, Ramakrishna S. Compos Sci Technol 2003;63:2223–53.
[6] Layman JM, Kenawy E-R, Watkins JR, Carr Jr ME, Bowlin G, Wnek GE. Polym Prepr 2003;44:94–5.
[7] Barris MA, Zelinka RL. US Patent No. 4,650,506. Issued March 17; 1987 to Donaldson Company, Inc.
[8] Chung HY, Hall JRB, Gogins MA, Crofoot DG, Weik TM. US Patent No. 6,743,273. Issued June 1; 2004 to Donaldson Company, Inc.
[9] Kenawy ER, Bowlin GL, Mansfield K, Layman J, Simpson DG, Sanders EH, et al. J Control Release 2002;81:57–64.
[10] Gibson P, Schreuder-Gibson H, Rivin D. Colloids Surf A 2001;187: 469–81.
[11] Schreuder-Gibson H, Gibson P, Senecal K, Sennett M, Walker J, Yeomans W, et al. J Adv Mater 2002;34:44–55.
[12] Boland ED, Matthews JA, Pawlowski KJ, Simpson DG, Wnek GE, Bowlin GL. Front Biosci 2004;9:1422–32.
[13] Matthews JA, Wnek GE, Simpson DG, Bowlin GL. Biomacromolecules 2002;3:232–8.
[14] Li WJ, Laurencin CT, Caterson EJ, Tuan RS, Ko FK. J Biomed Mater Res 2002;60:613–21.
[15] Taylor G. Proc R Soc London A, Mat Phys Sci 1964;280:383–97.
[16] Reneker DH, Yarin AL, Fong H, Koombhongse S. J Appl Phys 2000; 87:4531–47.
[17] Shin YM, Hohman MM, Brenner MP, Rutledge GC. Appl Phys Lett 2001;78:1149–51.
[18] Theron SA, Zussman E, Yarin AL. Polymer 2004;45:2017–30.
[19] Ferry JD. Viscoelastic properties of polymers. New York: Wiley; 1980 p. 641.
[20] Hohman MM, Shin M, Rutledge G, Brenner MP. Phys Fluids 2001; 13:2201–20.
[21] Hohman MM, Shin M, Rutledge G, Brenner MP. Phys Fluids 2001; 13:2221–36.
[22] Shin YM, Hohman MM, Brenner MP, Rutledge GC. Polymer 2001; 42:9955–67.
[23] Spivak AF, Dzenis YA. Appl Phys Lett 1998;73:3067–9.
[24] Spivak AF, Dzenis YA, Reneker DH. Mech Res Commun 2000;27: 37–42.
[25] Yarin AL, Koombhongse S, Reneker DH. J Appl Phys 2001;90: 4836–46.
[26] Yarin AL, Koombhongse S, Reneker DH. J Appl Phys 2001;89: 3018–26.
[27] Fridrikh SV, Yu JH, Brenner MP, Rutledge GC. Phys Rev Lett 2003; 90:144502.
[28] Feng JJ. Phys Fluids 2002;14:3912–26.
[29] Feng JJ. J Non-Newtonian Fluid Mech 2003;116:55–70.
[30] Larson RG, Sridhar T, Leal LG, McKinley GH, Likhtman AE, McLeish TCB. J Rheol 2003;47:809–18.
[31] Blades H, White JR. US Patent No. 3,081,519. Issued March 19; 1963 to E.I. du Pont de Nemours and Co.
[32] Shin H, Guckert JR, Kurian JV. US Patent No. 6,458,304. Issued October 1; 2002 to E.I. du Pont de Nemours and Co.
[33] Ziabicki A. Fundamentals of fibre formation: The science of fibre spinning and drawing. New York: Wiley; 1976. p. 488.
[34] Gou ZM, McHugh AJ. J Appl Polym Sci 2003;87:2136–45.
[35] Gou ZM, McHugh AJ. J Non-Newtonian Fluid Mech 2004;118: 121–36.
[36] Gupta P, Wilkes GL. Polymer 2003;44:6353–9.
[37] Jun Z, Hou HQ, Schaper A, Wendorff JH, Greiner A. E-Polymer 2003; No. 009.
[38] Kenawy ER, Layman JM, Watkins JR, Bowlin GL, Matthews JA, Simpson DG, et al. Biomaterials 2003;24:907–13.
[39] Stephens JS, Frisk S, Megelski S, Rabolt JF, Chase DB. Appl Spectrosc 2001;55:1287–90.
[40] McKee MG, Wilkes GL, Colby RH, Long TE. Macromolecules 2004; 37:1760–7.
[41] Graessley WW, editor. Advances in polymer science, vol. 16. New York: Springer; 1974. p. 179.
[42] Gandhi KS, Williams MC. J Appl Polym Sci 1972;16:2721–5.
[43] Bueche F. J Chem Phys 1956;25:599–600.
[44] Bueche F. J Polym Sci 1960;53:527–30.
[45] Festag R, Alexandratos SD, Joy DC, Wunderlich B, Annis B, Cook KD. J Am Soc Mass Spectrosc 1998;9:299–304.
[46] Festag R, Alexandratos SD, Cook KD, Joy DC, Annis B, Wunderlich B. Macromolecules 1997;30:6238–42.
[47] Griswold PD, Cuculo JA. J Appl Polym Sci 1974;18:2887–902.
[48] Megelski S, Stephens JS, Chase DB, Rabolt JF. Macromolecules 2002;35:8456–66.
[49] Deitzel JM, Kleinmeyer JD, Hirvonen JK, Tan NCB. Polymer 2001; 42:8163–70.
[50] Zong XH, Kim K, Fang DF, Ran SF, Hsiao BS, Chu B. Polymer 2002; 43:4403–12.
[51] Fetters LJ, Lohse DJ, Richter D, Witten TA, Zirkel A. Macromolecules 1994;27:4639–47.
[52] Cooper-White JJ, Mackay ME. J Polym Sci, B: Polym Phys 1999;37: 1803–14.
[53] Since M_e is a function of chain geometry, subtle changes in polymer structure (PLLA versus PDLA) can alter M_e. For example, the viscoelastic properties and, consequently, M_e, of syndiotactic polypropylene (PP) have been found to be quite different from atactic and isotactic PP (Ref. [54]). Still, in the absence of accurate $(M_e)_{PDLA}$ values, the assumption of equivalent entanglement molecular weights for PDLA and PLLA are more than likely reasonable to a first approximation
[54] Jones TD, Chaffin KA, Bates FS, Annis BK, Hagaman EW, Kim MH, et al. Macromolecules 2002;35:5061–8.
[55] Since PLLA was found to be insoluble in DMF, other solvents were examined. PLLA solutions were prepared using three different solvents: 5 wt% in DCM, 4 wt% in $CHCl_3$ (T_{BP} = 61 °C) and 4 wt% in 1,1,2,2-tetrachloroethane (TCE, T_{BP} = 147 °C). For the PLLA/TCE system, at 4 wt% mostly fibers with some beads were observed. In contrast, complete fibers are obtained from DCM (5 wt%) and $CHCl_3$ (4 wt%). The results are included in Table 2. It was also noticed that for the PLLA/TCE system, besides the beaded fibers, globular polymer droplets (100 μm) were observed, indicative of poor solubility. This is believed to be a result of the lower affinity of PLLA and TCE (in comparison to DCM and $CHCl_3$), which results in

a much slower dissolution rate of PLLA. In a subtle manner, though fibers are obtained, PLLA electrospinning is nevertheless affected by solvent quality

[56] Deitzel JM, Kleinmeyer J, Harris D, Tan NCB. Polymer 2001;42: 261–72.

[57] For details of the experimental setup see Ref. [38]. PEO (M_w = 2000k), PVP (M_w = 1300k), and EtOH (200 proof, HLPC grade) were all obtained from Aldrich and used as received. For the electrospinning experiment, a 0.4 wt% PEO solution in distilled deionized H_2O was prepared. PVP/EtOH solutions of different concentrations were also prepared (1, 3, 7 and 9 wt%—these concentrations were chosen based on theoretical predictions as discussed in the text). In a typical experiment, a solution of polymer (PEO/H_2O or PVP/EtOH) was drawn into a disposable polypropylene syringe equipped with a blunted stainless steel syringe tip. Employing a syringe pump (kdScientific, New Hope, PA) to generate a constant flow-rate (5 mL/h), the syringe tip was connected to a high voltage power supply (CZE 1000R, Spellman, NY). For the PEO/H_2O system, the field strength employed by Shin et al. (Ref. [22]) was employed: the applied voltage = 17 kV and the source-to-target distance = 20 cm. For the PVP/EtOH system, the source-to-target distance = 10 cm and an applied voltage of 10 kV was required for a jet of liquid to eject; consequently, an applied voltage = 12 kV was used in the PVP/EtOH experiments. Fibers for visualization by optical microscopy were collected on glass slides covering a grounded metal target rotating at approximately 300–500 rpm. Optical micrographs were obtained using an Olympus optical microscope (Olympus BE201).

[58] Yang Q, Li Z, Hong Y, Zhao Y, Wang C, Qiu S, et al. Polym Prepr 2003;44:173.

[59] Li D, Xia YN. Nano Lett 2003;3:555–60.

[60] Brandrup J, Immergut EH, Grulke EH. Polymer handbook. New York: Wiley; 1999.

[61] Tarazona MP, Saiz E. J Biochem Biophys Methods 2003;56:95–116.

[62] Obtained from the Pharmaceutical Technology Report(PTR-005-1) published by Hercules Incorporated.

[63] In our case fibers/beads are obtained for visualization by optical microscopy by collecting samples on glass slides covering a grounded metal target rotating at approximately 300–500 rpm. During imaging, the entire microscope slide is scanned for the presence of fibers, beaded fibers or just beads. In contrast, Yang et al. have mounted a TEM copper grid on top of an Al foil, which acts as the cathode. We believe there is a distinct possibility of underestimating the critical concentration required for complete fiber formation using this technique, since fibers will be preferentially trapped on the grid. This is especially true when the number of fibers having a beaded morphology is quite low as is the case in this system for solutions ranging from 5 to 7 wt%.

[64] Frisch HL, Simha R. In: Eirich FR, editor. Treatise on rheology, vol. 1. New York: Academic Press; 1956.

[65] Koski A, Yim K, Shivkumar S. Mater Lett 2004;58:493–7.

[66] Schreiber HP, Rudin A, Bagley EB. J Appl Polym Sci 1965;9:887–92.

[67] Hayahara T, Takao S. J Appl Polym Sci 1967;11:735–46.

[68] Hua CC, Yang CY. J Polym Res Taiwan 2002;9:79–90.

[69] Mead DW, Larson RG, Doi M. Macromolecules 1998;31:7895–914.

[70] Mhetar VR, Archer LA. J Polym Sci, B: Polym Phys 2000;38:222–33.

[71] Keller A. Faraday Discuss 1995;1–49.

[72] Rothstein JP, McKinley GH. J Non-Newtonian Fluid Mech 2002;108: 275–90.

[73] Basaran OA, Scriven LE. J Colloid Interface Sci 1990;140:10–30.

[74] Gonzalez H, Castellanos A. J Fluid Mech 1993;249:185–206.

[75] Yao L, Haas TW, Guiseppi-Elie A, Bowlin GL, Simpson DG, Wnek GE. Chem Mater 2003;15:1860–4.

[76] Fong H, Chun I, Reneker DH. Polymer 1999;40:4585–92.

[77] Bates WD, Barnes CP, Ounaies Z, Wnek GE. Polym Prepr 2003;44: 114.

[78] Tazaki M, Wada R, Okabe M, Homma T. Polym Bull 2000;44: 93–100.

[79] Young TH, Cheng LP, Hsieh CC, Chen LW. Macromolecules 1998; 31:1229–35.

[80] Bates WD, Shenoy SL, Wnek GE. In preparation.

[81] Bates WD. Unpublished results.

[82] McKee MG, Elkins CL, Long TE. Polymer 2004;45:8705–15.